

5-1-2002

Search for single-top-quark production in $p\bar{p}$ collisions at $\sqrt{s} = 1.8$ TeV

Darin Acosta

University of Florida, acosta@phys.ufl.edu

Kenneth A. Bloom

University of Nebraska - Lincoln, kbloom2@unl.edu

Collider Detector at Fermilab Collaboration

Follow this and additional works at: <http://digitalcommons.unl.edu/physicsbloom>

 Part of the [Physics Commons](#)

Acosta, Darin; Bloom, Kenneth A.; and Fermilab Collaboration, Collider Detector at, "Search for single-top-quark production in $p\bar{p}$ collisions at $\sqrt{s} = 1.8$ TeV" (2002). *Kenneth Bloom Publications*. 65.
<http://digitalcommons.unl.edu/physicsbloom/65>

This Article is brought to you for free and open access by the Research Papers in Physics and Astronomy at DigitalCommons@University of Nebraska - Lincoln. It has been accepted for inclusion in Kenneth Bloom Publications by an authorized administrator of DigitalCommons@University of Nebraska - Lincoln.

Search for single-top-quark production in $p\bar{p}$ collisions at $\sqrt{s}=1.8$ TeV

D. Acosta,¹ T. Affolder,² H. Akimoto,³ M. G. Albrow,⁴ P. Amaral,⁵ D. Ambrose,⁶ D. Amidei,⁷ K. Anikeev,⁸ J. Antos,⁹ G. Apollinari,⁴ T. Arisawa,³ A. Artikov,¹⁰ T. Asakawa,¹¹ W. Ashmanskas,⁵ F. Azfar,¹² P. Azzi-Bacchetta,¹³ N. Bacchetta,¹³ H. Bachacou,² S. Bailey,¹⁴ P. de Barbaro,¹⁵ A. Barbaro-Galtieri,² V. E. Barnes,¹⁶ B. A. Barnett,¹⁷ S. Baroian,¹⁸ M. Barone,¹⁹ G. Bauer,⁸ F. Bedeschi,²⁰ S. Belforte,²¹ W. H. Bell,²² G. Bellettini,²⁰ J. Bellinger,²³ D. Benjamin,²⁴ J. Bensinger,²⁵ A. Beretvas,⁴ J. P. Berge,⁴ J. Berryhill,⁵ A. Bhatti,²⁶ M. Binkley,⁴ D. Bisello,¹³ M. Bishai,⁴ R. E. Blair,²⁷ C. Blocker,²⁵ K. Bloom,⁷ B. Blumenfeld,¹⁷ S. R. Blusk,¹⁵ A. Bocci,²⁶ A. Bodek,¹⁵ G. Bolla,¹⁶ Y. Bonushkin,²⁸ D. Bortoletto,¹⁶ J. Boudreau,²⁹ A. Brandl,³⁰ S. van den Brink,¹⁷ C. Bromberg,³¹ M. Brozovic,²⁴ E. Brubaker,² N. Bruner,³⁰ E. Buckley-Geer,⁴ J. Budagov,¹⁰ H. S. Budd,¹⁵ K. Burkett,¹⁴ G. Busetto,¹³ A. Byon-Wagner,⁴ K. L. Byrum,²⁷ S. Cabrera,²⁴ P. Calafiura,² M. Campbell,⁷ W. Carithers,² J. Carlson,⁷ D. Carlsmith,²³ W. Caskey,¹⁸ A. Castro,³² D. Cauz,²¹ A. Cerri,²⁰ A. W. Chan,⁹ P. S. Chang,⁹ P. T. Chang,⁹ J. Chapman,⁷ C. Chen,⁶ Y. C. Chen,⁹ M.-T. Cheng,⁹ M. Chertok,¹⁸ G. Chiarelli,²⁰ I. Chirikov-Zorin,¹⁰ G. Chlachidze,¹⁰ F. Chlebana,⁴ L. Christofek,³³ M. L. Chu,⁹ J. Y. Chung,³⁴ Y. S. Chung,¹⁵ C. I. Ciobanu,³⁴ A. G. Clark,³⁵ A. P. Colijn,⁴ A. Connolly,² M. Convery,²⁶ J. Conway,³⁶ M. Cordelli,¹⁹ J. Cranshaw,³⁷ R. Culbertson,⁴ D. Dagenhart,³⁸ S. D'Auria,²² F. DeJongh,⁴ S. Dell'Agnello,¹⁹ M. Dell'Orso,²⁰ S. Demers,¹⁵ L. Demortier,²⁶ M. Deninno,³² P. F. Derwent,⁴ T. Devlin,³⁶ J. R. Dittmann,⁴ A. Dominguez,² S. Donati,²⁰ J. Done,³⁹ M. D'Onofrio,²⁰ T. Dorigo,¹⁴ N. Eddy,³³ K. Einsweiler,² J. E. Elias,⁴ E. Engels, Jr.,²⁹ R. Erbacher,⁴ D. Errede,³³ S. Errede,³³ Q. Fan,¹⁵ H.-C. Fang,² R. G. Feild,⁴⁰ J. P. Fernandez,⁴ C. Ferretti,²⁰ R. D. Field,¹ I. Fiori,³² B. Flaughner,⁴ G. W. Foster,⁴ M. Franklin,¹⁴ J. Freeman,⁴ J. Friedman,⁸ Y. Fukui,⁴¹ I. Furic,⁸ S. Galeotti,²⁰ A. Gallas,^{14,*} M. Gallinaro,²⁶ T. Gao,⁶ M. Garcia-Sciveres,² A. F. Garfinkel,¹⁶ P. Gatti,¹³ C. Gay,⁴⁰ D. W. Gerdes,⁷ P. Giannetti,²⁰ M. P. Giordani,¹⁸ P. Giromini,¹⁹ V. Glagolev,¹⁰ D. Glenzinski,⁴ M. Gold,³⁰ J. Goldstein,⁴ I. Gorelov,³⁰ A. T. Goshaw,²⁴ Y. Gotra,²⁹ K. Goulianos,²⁶ C. Green,¹⁶ G. Grim,¹⁸ P. Gris,⁴ C. Grosso-Pilcher,⁵ M. Guenther,¹⁶ G. Guillian,⁷ J. Guimaraes da Costa,¹⁴ R. M. Haas,¹ C. Haber,² S. R. Hahn,⁴ C. Hall,¹⁴ T. Handa,⁴² R. Handler,²³ W. Hao,³⁷ F. Happacher,¹⁹ K. Hara,¹¹ A. D. Hardman,¹⁶ R. M. Harris,⁴ F. Hartmann,⁴³ K. Hatakeyama,²⁶ J. Hauser,²⁸ J. Heinrich,⁶ A. Heiss,⁴³ M. Herndon,¹⁷ C. Hill,¹⁸ A. Hocker,¹⁵ K. D. Hoffman,¹⁶ R. Hollebeek,⁶ L. Holloway,³³ B. T. Huffman,¹² R. Hughes,³⁴ J. Huston,³¹ J. Huth,¹⁴ H. Ikeda,¹¹ J. Incandela,^{4,†} G. Introzzi,²⁰ A. Ivanov,¹⁵ J. Iwai,³ Y. Iwata,⁴² E. James,⁷ M. Jones,⁶ U. Joshi,⁴ H. Kambara,³⁵ T. Kamon,³⁹ T. Kaneko,¹¹ M. Karagoz Unel,^{39,*} K. Karr,³⁸ S. Kartal,⁴ H. Kasha,⁴⁰ Y. Kato,⁴⁴ T. A. Keaffaber,¹⁶ K. Kelley,⁸ M. Kelly,⁷ D. Khazins,²⁴ T. Kikuchi,¹¹ B. Kilminster,¹⁵ B. J. Kim,⁴⁵ D. H. Kim,⁴⁵ H. S. Kim,³³ M. J. Kim,⁴⁵ S. B. Kim,⁴⁵ S. H. Kim,¹¹ Y. K. Kim,² M. Kirby,²⁴ M. Kirk,²⁵ L. Kirsch,²⁵ S. Klimentenko,¹ P. Koehn,³⁴ K. Kondo,³ J. Konigsberg,¹ A. Korn,⁸ A. Korytov,¹ E. Kovacs,²⁷ J. Kroll,⁶ M. Kruse,²⁴ S. E. Kuhlmann,²⁷ K. Kurino,⁴² T. Kuwabara,¹¹ A. T. Laasanen,¹⁶ N. Lai,⁵ S. Lami,²⁶ S. Lammel,⁴ J. Lancaster,²⁴ M. Lancaster,² R. Lander,¹⁸ A. Lath,³⁶ G. Latino,²⁰ T. LeCompte,²⁷ K. Lee,³⁷ S. Leone,²⁰ J. D. Lewis,⁴ M. Lindgren,²⁸ T. M. Liss,³³ J. B. Liu,¹⁵ Y. C. Liu,⁹ D. O. Litvintsev,⁴ O. Lobban,³⁷ N. S. Lockyer,⁶ J. Loken,¹² M. Loreti,¹³ D. Lucchesi,¹³ P. Lukens,⁴ S. Lusin,²³ L. Lyons,¹² J. Lys,² R. Madrak,¹⁴ K. Maeshima,⁴ P. Maksimovic,¹⁴ L. Malferrari,³² M. Mangano,²⁰ M. Mariotti,¹³ G. Martignon,¹³ A. Martin,⁴⁰ J. A. J. Matthews,³⁰ P. Mazzanti,³² K. S. McFarland,¹⁵ P. McIntyre,³⁹ M. Menguzzato,¹³ A. Menzione,²⁰ P. Merkel,⁴ C. Mesropian,²⁶ A. Meyer,⁴ T. Miao,⁴ R. Miller,³¹ J. S. Miller,⁷ H. Minato,¹¹ S. Miscetti,¹⁹ M. Mishina,⁴¹ G. Mitselmakher,¹ Y. Miyazaki,⁴⁴ N. Moggi,³² E. Moore,³⁰ R. Moore,⁷ Y. Morita,⁴¹ T. Moulik,¹⁶ M. Mulhearn,⁸ A. Mukherjee,⁴ T. Muller,⁴³ A. Munar,²⁰ P. Murat,⁴ S. Murgia,³¹ J. Nachtman,²⁸ V. Nagaslaev,³⁷ S. Nahn,⁴⁰ H. Nakada,¹¹ I. Nakano,⁴² C. Nelson,⁴ T. Nelson,⁴ C. Neu,³⁴ D. Neuberger,⁴³ C. Newman-Holmes,⁴ C.-Y. P. Ngan,⁸ H. Niu,²⁵ L. Nodulman,²⁷ A. Nomerotski,¹ S. H. Oh,²⁴ Y. D. Oh,⁴⁵ T. Ohmoto,⁴² T. Ohsugi,⁴² R. Oishi,¹¹ T. Okusawa,⁴⁴ J. Olsen,²³ W. Orejudos,² C. Pagliarone,²⁰ F. Palmonari,²⁰ R. Paoletti,²⁰ V. Papadimitriou,³⁷ D. Partos,²⁵ J. Patrick,⁴ G. Pauletta,²¹ M. Paulini,^{2,‡} C. Paus,⁸ D. Pellett,¹⁸ L. Pescara,¹³ T. J. Phillips,²⁴ G. Piacentino,²⁰ K. T. Pitts,³³ A. Pompos,¹⁶ L. Pondrom,²³ G. Pope,²⁹ F. Prokoshin,¹⁰ J. Proudfoot,²⁷ F. Ptohos,¹⁹ O. Pukhov,¹⁰ G. Punzi,²⁰ A. Rakitine,⁸ F. Ratnikov,³⁶ D. Reher,² A. Reichold,¹² P. Renton,¹² A. Ribon,¹³ W. Riegler,¹⁴ F. Rimondi,³² L. Ristori,²⁰ M. Riveline,⁴⁶ W. J. Robertson,²⁴ T. Rodrigo,⁴⁷ S. Rolli,³⁸ L. Rosenson,⁸ R. Roser,⁴ R. Rossin,¹³ C. Rott,¹⁶ A. Roy,¹⁶ A. Ruiz,⁴⁷ A. Safonov,¹⁸ R. St. Denis,²² W. K. Sakumoto,¹⁵ D. Saltzberg,²⁸ C. Sanchez,³⁴ A. Sansoni,¹⁹ L. Santi,²¹ H. Sato,¹¹ P. Savard,⁴⁶ A. Savoy-Navarro,⁴ P. Schlabach,⁴ E. E. Schmidt,⁴ M. P. Schmidt,⁴⁰ M. Schmitt,^{14,*} L. Scodellaro,¹³ A. Scott,²⁸ A. Scribano,²⁰ A. Sedov,¹⁶ S. Segler,⁴ S. Seidel,³⁰ Y. Seiya,¹¹ A. Semenov,¹⁰ F. Semeria,³² T. Shah,⁸ M. D. Shapiro,² P. F. Shepard,²⁹ T. Shibayama,¹¹ M. Shimojima,¹¹ M. Shochet,⁵ A. Sidoti,¹³ J. Siegrist,² A. Sill,³⁷ P. Sinervo,⁴⁶ P. Singh,³³ A. J. Slaughter,⁴⁰ K. Sliwa,³⁸ C. Smith,¹⁷ F. D. Snider,⁴ A. Solodsky,²⁶ J. Spalding,⁴ T. Speer,³⁵ P. Sphicas,⁸ F. Spinella,²⁰ M. Spiropulu,⁵ L. Spiegel,⁴ J. Steele,²³ A. Stefanini,²⁰ J. Strogas,³³ F. Strumia,³⁵ D. Stuart,⁴ K. Sumorok,⁸ T. Suzuki,¹¹ T. Takano,⁴⁴ R. Takashima,⁴² K. Takikawa,¹¹ P. Tamburello,²⁴ M. Tanaka,¹¹ B. Tannenbaum,²⁸ M. Tecchio,⁷ R. J. Tesarek,⁴ P. K. Teng,⁹ K. Terashi,²⁶ S. Tether,⁸ A. S. Thompson,²² E. Thomson,³⁴ R. Thurman-Keup,²⁷ P. Tipton,¹⁵ S. Tkaczyk,⁴ D. Toback,³⁹ K. Tollefson,¹⁵ A. Tollestrup,⁴ D. Tonelli,²⁰ H. Toyoda,⁴⁴ W. Trischuk,⁴⁶ J. F. de Troconiz,¹⁴ J. Tseng,⁸ D. Tsybychev,⁴ N. Turini,²⁰ F. Ukegawa,¹¹ T. Vaiculis,¹⁵ J. Valls,³⁶ S. Vejck III,⁴ G. Velev,⁴ G. Veramendi,² R. Vidal,⁴ I. Vila,⁴⁷ R. Vilar,⁴⁷ I. Volobouev,² M. von der Mey,²⁸ D. Vucinic,⁸ R. G. Wagner,²⁷ R. L. Wagner,⁴ N. B. Wallace,³⁶ Z. Wan,³⁶

C. Wang,²⁴ M. J. Wang,⁹ S. M. Wang,¹ B. Ward,²² S. Waschke,²² T. Watanabe,¹¹ D. Waters,¹² T. Watts,³⁶ R. Webb,³⁹ H. Wenzel,⁴³ W. C. Wester III,⁴ A. B. Wicklund,²⁷ E. Wicklund,⁴ T. Wilkes,¹⁸ H. H. Williams,⁶ P. Wilson,⁴ B. L. Winer,³⁴ D. Winn,⁷ S. Wolbers,⁴ D. Wolinski,⁷ J. Wolinski,³¹ S. Wolinski,⁷ S. Worm,³⁶ X. Wu,³⁵ J. Wyss,²⁰ W. Yao,² G. P. Yeh,⁴ P. Yeh,⁹ J. Yoh,⁴ C. Yosef,³¹ T. Yoshida,⁴⁴ I. Yu,⁴⁵ S. Yu,⁶ Z. Yu,⁴⁰ A. Zanetti,²¹ and F. Zetti²

(CDF Collaboration)

¹*University of Florida, Gainesville, Florida 32611*

²*Ernest Orlando Lawrence Berkeley National Laboratory, Berkeley, California 94720*

³*Waseda University, Tokyo 169, Japan*

⁴*Fermi National Accelerator Laboratory, Batavia, Illinois 60510*

⁵*Enrico Fermi Institute, University of Chicago, Chicago, Illinois 60637*

⁶*University of Pennsylvania, Philadelphia, Pennsylvania 19104*

⁷*University of Michigan, Ann Arbor, Michigan 48109*

⁸*Massachusetts Institute of Technology, Cambridge, Massachusetts 02139*

⁹*Institute of Physics, Academia Sinica, Taipei, Taiwan 11529, Republic of China*

¹⁰*Joint Institute for Nuclear Research, RU-141980 Dubna, Russia*

¹¹*University of Tsukuba, Tsukuba, Ibaraki 305, Japan*

¹²*University of Oxford, Oxford OX1 3RH, United Kingdom*

¹³*Universita di Padova, Istituto Nazionale di Fisica Nucleare, Sezione di Padova, I-35131 Padova, Italy*

¹⁴*Harvard University, Cambridge, Massachusetts 02138*

¹⁵*University of Rochester, Rochester, New York 14627*

¹⁶*Purdue University, West Lafayette, Indiana 47907*

¹⁷*The Johns Hopkins University, Baltimore, Maryland 21218*

¹⁸*University of California at Davis, Davis, California 95616*

¹⁹*Laboratori Nazionali di Frascati, Istituto Nazionale di Fisica Nucleare, I-00044 Frascati, Italy*

²⁰*Istituto Nazionale di Fisica Nucleare, University and Scuola Normale Superiore of Pisa, I-56100 Pisa, Italy*

²¹*Istituto Nazionale di Fisica Nucleare, University of Trieste, I-34127 Trieste, and University of Udine, I-33100 Udine, Italy*

²²*Glasgow University, Glasgow G12 8QQ, United Kingdom*

²³*University of Wisconsin, Madison, Wisconsin 53706*

²⁴*Duke University, Durham, North Carolina 27708*

²⁵*Brandeis University, Waltham, Massachusetts 02254*

²⁶*Rockefeller University, New York, New York 10021*

²⁷*Argonne National Laboratory, Argonne, Illinois 60439*

²⁸*University of California at Los Angeles, Los Angeles, California 90024*

²⁹*University of Pittsburgh, Pittsburgh, Pennsylvania 15260*

³⁰*University of New Mexico, Albuquerque, New Mexico 87131*

³¹*Michigan State University, East Lansing, Michigan 48824*

³²*Istituto Nazionale di Fisica Nucleare, University of Bologna, I-40127 Bologna, Italy*

³³*University of Illinois, Urbana, Illinois 61801*

³⁴*The Ohio State University, Columbus, Ohio 43210*

³⁵*University of Geneva, CH-1211 Geneva 4, Switzerland*

³⁶*Rutgers University, Piscataway, New Jersey 08855*

³⁷*Texas Tech University, Lubbock, Texas 79409*

³⁸*Tufts University, Medford, Massachusetts 02155*

³⁹*Texas A&M University, College Station, Texas 77843*

⁴⁰*Yale University, New Haven, Connecticut 06520*

⁴¹*High Energy Accelerator Research Organization (KEK), Tsukuba, Ibaraki 305, Japan*

⁴²*Hiroshima University, Higashi-Hiroshima 724, Japan*

⁴³*Institut für Experimentelle Kernphysik, Universität Karlsruhe, 76128 Karlsruhe, Germany*

⁴⁴*Osaka City University, Osaka 588, Japan*

⁴⁵*Center for High Energy Physics Kyungpook National University, Taegu 702-701,*

Seoul National University, Seoul 151-742,

and SungKyunKwan University, Suwon 440-746, Korea

⁴⁶*Institute of Particle Physics, University of Toronto, Toronto M5S 1A7, Canada*

⁴⁷*Instituto de Fisica de Cantabria, CSIC-University of Cantabria, 39005 Santander, Spain*

(Received 12 October 2001; published 23 April 2002)

We search for standard model single-top-quark production in the W -gluon fusion and W^* channels using 106 pb^{-1} of data from $p\bar{p}$ collisions at $\sqrt{s}=1.8 \text{ TeV}$ collected with the Collider Detector at Fermilab. We set an upper limit at 95% confidence level (C.L.) on the combined W -gluon fusion and W^* single-top cross section of 14 pb, roughly six times larger than the standard model prediction. Separate 95% C.L. upper limits in the W -gluon fusion and W^* channels are also determined and are found to be 13 and 18 pb, respectively.

DOI: 10.1103/PhysRevD.65.091102

PACS number(s): 14.65.Ha, 12.15.Ji, 13.85.Rm

The observation of the top quark in $p\bar{p}$ collisions at the Fermilab Tevatron has relied on pair production through the strong interaction, typically $q\bar{q} \rightarrow t\bar{t}$. A top quark can also be produced singly, in association with a b quark, through the electroweak interaction [1]. The two dominant “single-top” processes are “ Wg ” (i.e. W -gluon fusion, $qg \rightarrow t\bar{b}q'$) and “ W^* ” ($q\bar{q}' \rightarrow t\bar{b}$). Within the context of the standard model, a measurement of the rate of these processes at a hadron collider allows a determination of the Cabibbo-Kobayashi-Maskawa matrix element V_{tb} [2]. Assuming $|V_{tb}|=1$, the predicted cross sections for Wg and W^* are 1.7 pb [3] and 0.7 pb [4], respectively, compared to 5.1 pb for $t\bar{t}$ pair production [5]. The DØ Collaboration has recently published 95% confidence level (C.L.) upper limits of 22 pb on Wg and 17 pb on W^* production [6]. In this Rapid Communication we report on two searches: one for the two single-top processes combined, and the other for each process separately.

The expected final state of a single-top event consists of W -decay products plus two or more jets, including one b -quark jet from the decay of the top quark. In W^* events, we expect a second b -quark jet from the $W^*t\bar{b}$ vertex. In Wg events, a second jet originates from the recoiling light quark and a third jet is produced through the splitting of the initial-state gluon into $b\bar{b}$. This b -quark jet is produced at a larger absolute value of pseudorapidity [7] and lower transverse momentum than the second b -quark jet in W^* events [1].

Single-top processes are harder to observe than $t\bar{t}$ production because their cross section is smaller and their final state, containing fewer jets, competes with a larger W +multijet background from QCD. *A priori* we do not expect sensitivity to the standard model cross section in the presently available data. However, a number of new physics processes could enhance the single-top production rate, motivating a search [8–10]. For example, current Collider Detector at Fermilab (CDF) data are expected to be sensitive to a new flavor gauge boson with mass below $1 \text{ TeV}/c^2$ [9].

Our measurement uses $106 \pm 4 \text{ pb}^{-1}$ of data from $p\bar{p}$ collisions at $\sqrt{s}=1.8 \text{ TeV}$ collected with the Collider Detector at Fermilab between 1992 and 1995 (“run I”). The detector is described in detail elsewhere [11]. We restrict our single-

top search to events with evidence of a leptonic W decay: an isolated [12] electron (muon) candidate with $E_T(P_T) > 20 \text{ GeV}(\text{GeV}/c)$ and missing transverse energy [13] $\cancel{E}_T > 20 \text{ GeV}$ from the neutrino. We remove events that were identified in a previous CDF analysis [14] as $t\bar{t}$ dilepton candidates. Events with a second, same-flavor and opposite-charge lepton that forms an invariant mass with the first lepton between 75 and 105 GeV/c^2 are rejected as likely to have come from Z^0 boson decays. Furthermore, to reject those dilepton $t\bar{t}$ or Z^0 candidates where one lepton fails our electron or muon identification, we also remove events that contain a track with $P_T > 15 \text{ GeV}/c$ and charge opposite that of the primary lepton, and such that the total P_T of all tracks in a cone of radius $\Delta R \equiv \sqrt{\Delta\eta^2 + \Delta\phi^2} = 0.4$ around this track is less than 2 GeV/c [15]. Jets are formed as clusters of calorimeter towers within cones of fixed radius $\Delta R = 0.4$. Events are required to have one, two, or three jets with $E_T > 15 \text{ GeV}$ and $|\eta| < 2.0$; at least one jet must be identified as likely to contain a b quark (“ b -tagged”) using displaced-vertex information from the silicon vertex detector (SVX) [15]. If a second jet in the event is also b -tagged, either in the SVX or by the presence of a soft lepton indicative of semi-leptonic b decay, the event is labeled “double-tag,” otherwise it is labeled “single-tag.” The above event selection cuts are common to our combined and separate searches for the two single-top processes. Additional cuts are applied within each analysis.

We first describe our search for single-top production in the Wg and W^* channels combined. The expected signal significance is improved by requiring the invariant mass $M_{l\nu b}$, reconstructed from the lepton, neutrino, and highest- E_T b -tagged jet, to lie in a window around the top quark mass, $140 < M_{l\nu b} < 210 \text{ GeV}/c^2$. The neutrino momentum is obtained from the \cancel{E}_T and the constraint that $M_{l\nu} = M_W$ [16]. The variable $M_{l\nu b}$ discriminates against both non-top and $t\bar{t}$ backgrounds, in the latter case because combinatorial errors in assigning partons to final-state jets broaden the $M_{l\nu b}$ distribution compared to single top.

We determine the efficiency of our selection criteria from events generated by the PYTHIA Monte Carlo program [17] and subjected to a CDF detector simulation. The acceptance times branching ratio is $(1.7 \pm 0.3)\%$ for each of the two single-top processes. The largest contributions to the acceptance uncertainties come from lepton triggering and identification (10%), and b -tagging (10%). Combining these acceptances with the cross sections predicted by theory [3,4] and the size of the CDF Run I dataset, we expect a total signal yield of 4.3 events.

*Present address: Northwestern University, Evanston, IL 60208.

†Present address: University of California, Santa Barbara, CA 93106.

‡Present address: Carnegie Mellon University, Pittsburgh, PA 15213.

TABLE I. Expected numbers of signal and background events passing all cuts in the W +jets data sample, compared with observations. The uncertainties on the expected numbers of single-top events do not include uncertainties on the theoretical cross section calculations.

| Process | Combined search | Separate search | |
|------------|-----------------|-----------------|-----------------|
| | $W+1,2,3$ jets | Single-tag | Double-tag |
| Wg | 3.0 ± 0.6 | 1.4 ± 0.3 | 0.04 ± 0.01 |
| W^* | 1.3 ± 0.2 | 0.55 ± 0.15 | 0.32 ± 0.06 |
| $t\bar{t}$ | 8.4 ± 2.7 | 1.4 ± 0.5 | 0.7 ± 0.2 |
| non-top | 54 ± 12 | 10 ± 2 | 1.6 ± 0.4 |
| Total | 67 ± 12 | 14 ± 2 | 2.7 ± 0.5 |
| Observed | 65 | 15 | 6 |

Expectations for signal and background rates are listed in the second column of Table I. We estimate the $t\bar{t}$ background from a HERWIG Monte Carlo calculation [18] followed by a detector simulation. Normalizing to the theoretically predicted cross section, $\sigma_{t\bar{t}} = 5.1 \pm 0.9$ pb [5], we expect 8.4 ± 2.7 $t\bar{t}$ events to survive our selection criteria, where the uncertainty includes theoretical and acceptance contributions.

The largest component of the non- $t\bar{t}$ background in the SVX-tagged W +jets sample is inclusive W production in association with heavy-flavor jets (e.g. $p\bar{p} \rightarrow Wg$, followed by $g \rightarrow b\bar{b}$). Additional sources include ‘‘mistags,’’ in which a light-quark jet is erroneously identified as heavy flavor, ‘‘non- W ’’ (e.g. direct $b\bar{b}$ production), and smaller contributions from WW, WZ , and Z +heavy-flavor [15]. The mistag and non- W rates are estimated from data, the

TABLE II. Systematic uncertainties on the fit result for β_s in the combined search ($Wg+W^*$), and for β_{Wg} and β_{W^*} in the separate search (see text). The δn columns list fractional uncertainties due to signal normalization effects and the ΔS columns list absolute uncertainties due to effects on the shapes of the fitted distributions.

| Source | $Wg+W^*$ | | Wg | | W^* | |
|-----------------------------------|------------|------------|------------|------------|------------|------------|
| | δn | ΔS | δn | ΔS | δn | ΔS |
| Jet E_T scale | 0.01 | 0.25 | 0.01 | 0.02 | 0.01 | 0.06 |
| Initial-state radiation | 0.02 | 0.15 | 0.06 | 0.07 | 0.06 | 0.13 |
| Final-state radiation | 0.03 | 0.02 | 0.07 | 0.02 | 0.05 | 0.01 |
| Parton distributions | 0.04 | 0.02 | 0.01 | 0.03 | 0.01 | 0.02 |
| Signal generator | 0.02 | 0.25 | 0.08 | 0.03 | 0.07 | 0.12 |
| Background model | - | 0.04 | - | 0.12 | - | 0.18 |
| Top mass | 0.04 | 0.01 | 0.01 | 0.12 | 0.00 | 0.35 |
| Trigger and lepton identification | 0.10 | - | 0.10 | - | 0.10 | - |
| b -tag efficiency | 0.10 | - | 0.10 | - | 0.10 | - |
| Luminosity | 0.04 | - | 0.04 | - | 0.04 | - |
| Total | 0.16 | 0.39 | 0.19 | 0.19 | 0.18 | 0.44 |

W +heavy-flavor rates from Monte Carlo normalized to data, and the smaller sources such as diboson production from Monte Carlo normalized to theory predictions [15]. The total non-top background expectation is 54 ± 12 events. The uncertainty on our background includes the effect of varying the top mass by its uncertainty of ± 5 GeV/ c^2 .

To measure the combined $Wg + W^*$ single-top production cross section, we use a kinematic variable whose distribution is very similar for the two single-top processes and is different for background processes: the scalar sum H_T of E_T and the transverse energies of the lepton and all jets in the event. We perform an unbinned maximum-likelihood fit of the H_T distribution from data to a linear superposition of the expected H_T distributions from single-top signal, $t\bar{t}$ and non-top backgrounds. We model the shape of the H_T distribution for all sources of non-top background with VECBOS-generated [19] events containing a W plus two partons that we force to be a $b\bar{b}$ pair. We have checked that VECBOS reproduces the H_T and $M_{l\nu b}$ distributions for the b -tagged $W+1$ -jet data before the $M_{l\nu b}$ cut, a sample in which the non-top backgrounds are expected to dominate. In the search sample, the observed H_T distribution agrees with the spectrum derived from Monte Carlo calculations when the latter are normalized to the *a priori* predicted numbers of events (Fig. 1).

We set an upper limit on the cross section using the likelihood function

$$\mathcal{L}(\beta_s, \beta_{t\bar{t}}, \beta_{nt}) = G_1(\beta_{t\bar{t}})G_2(\beta_{nt})\mathcal{L}_{\text{shape}}(\beta_s, \beta_{t\bar{t}}, \beta_{nt}),$$

where $\beta_s, \beta_{t\bar{t}}$ and β_{nt} are fit parameters representing, respectively, factors by which the standard model cross section predictions for single-top, $t\bar{t}$ and non-top must be multiplied to fit the data. The functions G_1 and G_2 are Gaussian densities constraining the background factors $\beta_{t\bar{t}}$ and β_{nt} to unity, and $\mathcal{L}_{\text{shape}}$ represents the joint probability density for observing the N_{obs} data events at their respective values of H_T :

$$\mathcal{L}_{\text{shape}}(\beta_s, \beta_{t\bar{t}}, \beta_{nt}) = \frac{\mu_{\text{fit}}^{N_{\text{obs}}} e^{-\mu_{\text{fit}} N_{\text{obs}}}}{N_{\text{obs}}!} \prod_{i=1}^{N_{\text{obs}}} \frac{\beta_s F_s(H_{Ti}) + \beta_{t\bar{t}} F_{t\bar{t}}(H_{Ti}) + \beta_{nt} F_{nt}(H_{Ti})}{\mu_{\text{fit}}}.$$

In this expression, $\mu_{\text{fit}} \equiv \beta_s \mu_s + \beta_{t\bar{t}} \mu_{t\bar{t}} + \beta_{nt} \mu_{nt}$, where $\mu_s, \mu_{t\bar{t}}$ and μ_{nt} are the predicted numbers of events, and $F(H_T)$ are smoothed H_T distributions for signal and background, normalized to unity. The maximum of \mathcal{L} is obtained for $\beta_s = 2.0 \pm 1.8$, where the uncertainty is statistical only and includes the effect of correlations with the other fit parameters.

To extract Bayesian upper limits on the single-top production rate, we construct a probability distribution $f(\beta_s)$ by maximizing $\mathcal{L}(\beta_s, \beta_{t\bar{t}}, \beta_{nt})$ with respect to $\beta_{t\bar{t}}$ and β_{nt} for each value of β_s , and multiplying the result with a flat prior distribution for β_s . We then convolute $f(\beta_s)$ with two Gaussian smearing functions. The first one has width $\beta_s \delta n$, where δn is the sum in quadrature of all the normalization uncertainties listed in Table II. The width of the second smearing Gaussian is the sum in quadrature of all the sys-

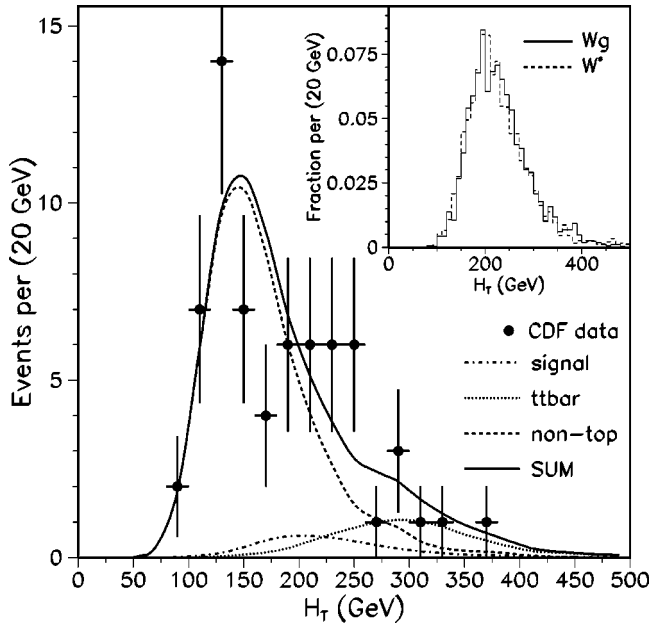


FIG. 1. The H_T distribution for data in the combined search, compared with smoothed Monte Carlo predictions for signal and backgrounds (second column in Table I). H_T is the scalar sum of E_T and the transverse energies of the lepton and all jets in the event. The inset shows that the Monte Carlo modeling of H_T is very similar for both signal processes.

tematic uncertainties relative to the shape of the H_T distribution (ΔS in Table II). Finally, the smeared distribution is integrated to find the 95% C.L. upper limit on single-top production. We find this limit to be $\beta_s^{95} = 5.9$, corresponding to a cross section of 14 pb.

Because of significant differences in the final-state kinematics of the two single-top processes, it is possible to search for them separately. This is interesting, because an exotic single-top production mechanism may contribute to one and not the other, for example a heavy W' decaying to a $t\bar{b}$ quark pair adding to the apparent W^* rate [10]. For the separated search, we use events in the $W+2$ -jets sample only and consider two non-overlapping subsamples. The first one consists of single-tag events in which the reconstructed top mass lies in the window $145 < M_{l\nu b} < 205$ GeV/ c^2 , and the second consists of double-tag events. The expected compositions, calculated in the same way as for the combined analysis, are shown in the last two columns of Table I: in the single-tag sample, Wg is about 2.5 times larger than W^* ; in the double-tag sample, W^* is about 7.5 times larger than Wg .

The Wg component in the single-tag sample can be measured by considering that the light-quark jet in Wg events is about twice as likely to be in the same hemisphere as the outgoing (anti)proton beam when a top (anti)quark is produced. Thus the product $Q \times \eta$ of the primary lepton charge and the untagged jet pseudorapidity has a strongly asymmetric distribution. In the double-tag sample, the W^* component can be extracted from the distribution of $M_{l\nu b}$. In this case, since both jets are tagged, the b -jet with the largest η ($-\eta$) is used in forming $M_{l\nu b}$ for a $t(\bar{t})$ decay, as determined by the sign of the primary lepton in the event, an

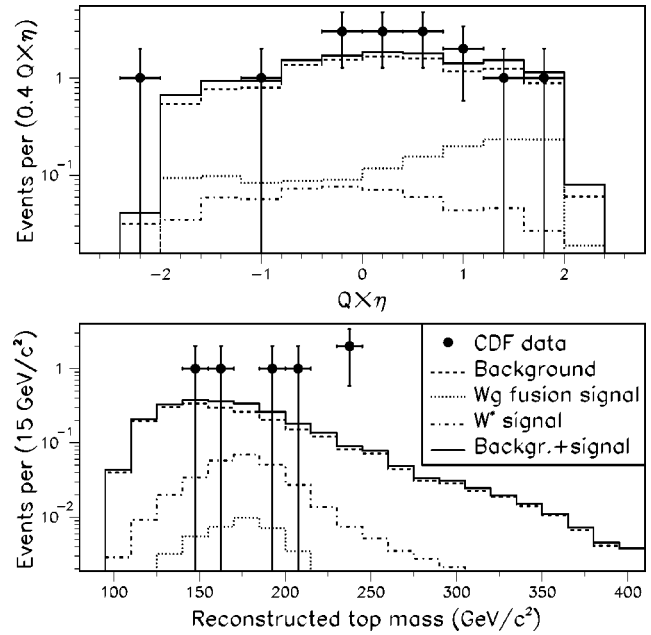


FIG. 2. Top: distribution of the product $Q \times \eta$ of the lepton charge and the untagged jet pseudorapidity for single-tag $W+2$ -jets events. Bottom: distribution of the reconstructed top mass for double-tag events. The data are compared with expectations for signal and backgrounds (third and fourth columns in Table I).

assignment that is expected to be correct 64% of the time. The $Q \times \eta$ and $M_{l\nu b}$ distributions for the data are compared to expectations for signal and background in Fig. 2. For the separate Wg and W^* searches, we use a HERWIG Monte Carlo calculation to model our signals.

A binned maximum-likelihood fit is used to extract the amounts of Wg and W^* present in the $W+2$ -jets data. The likelihood function has the following form:

$$\begin{aligned} \mathcal{L}(\beta_{Wg}, \beta_{W^*}, \beta_{t\bar{t}1}, \beta_{t\bar{t}2}, \beta_{nt1}, \beta_{nt2}) \\ = G_1(\beta_{t\bar{t}1}) G_2(\beta_{nt1}) \mathcal{L}_1(\beta_{Wg}, \beta_{W^*}, \beta_{t\bar{t}1}, \beta_{nt1}) \\ \times G_3(\beta_{t\bar{t}2}) G_4(\beta_{nt2}) \mathcal{L}_2(\beta_{Wg}, \beta_{W^*}, \beta_{t\bar{t}2}, \beta_{nt2}), \end{aligned}$$

where the fit parameters are factors by which the predicted numbers of Wg (β_{Wg}), W^* (β_{W^*}), single-tag $t\bar{t}$ ($\beta_{t\bar{t}1}$), double-tag $t\bar{t}$ ($\beta_{t\bar{t}2}$), single-tag non-top (β_{nt1}) and double-tag non-top (β_{nt2}) events must be multiplied to fit the data. The G_i functions are Gaussian constraints on the normalizations of the various backgrounds, \mathcal{L}_1 is a binned Poisson likelihood for the $Q \times \eta$ distribution of single-tag events, and \mathcal{L}_2 is a binned Poisson likelihood for the $M_{l\nu b}$ distribution of double-tag events.

The result of the maximum-likelihood fit for the single-top content of the data is $-0.6_{-4.0}^{+4.8} Wg$ events and $7.6_{-4.8}^{+5.9} W^*$ events. The systematic uncertainties are listed in Table II. We extract upper limits on the individual single-top processes in the same way as for the combined search. At the 95% C.L., we find upper limits of 13 and 18 pb on single-top

production in the Wg and W^* channels, respectively. These two limits are correlated since they are derived from the same likelihood function.

In summary, we conclude that electroweak $t\bar{b}$ production is out of reach in the Run I CDF data set. At the 95% C.L., we set an upper limit on the combined $Wg + W^*$ single-top cross section of 14 pb. Separate 95% C.L. upper limits in the Wg and W^* channels are 13 and 18 pb, respectively.

We thank the Fermilab staff and the technical staffs of the participating institutions for their vital contributions. This

work was supported by the U.S. Department of Energy and National Science Foundation; the Italian Istituto Nazionale di Fisica Nucleare; the Ministry of Education, Culture, Sports, Science, and Technology of Japan; the Natural Sciences and Engineering Research Council of Canada; the National Science Council of the Republic of China; the Swiss National Science Foundation; the A. P. Sloan Foundation; the Bundesministerium fuer Bildung und Forschung, Germany; the Korea Science and Engineering Foundation (KoSEF); the Korea Research Foundation; and the Comision Interministerial de Ciencia y Tecnologia, Spain.

-
- [1] S.S.D. Willenbrock and D.A. Dicus, Phys. Rev. D **34**, 155 (1986); S. Dawson and S. Willenbrock, Nucl. Phys. **B284**, 449 (1987); C.-P. Yuan, Phys. Rev. D **41**, 42 (1990); R.K. Ellis and S. Parke, *ibid.* **46**, 3785 (1992); D. Carlson and C.-P. Yuan, Phys. Lett. B **306**, 386 (1993).
- [2] T. Stelzer and S. Willenbrock, Phys. Lett. B **357**, 125 (1995).
- [3] T. Stelzer, Z. Sullivan, and S. Willenbrock, Phys. Rev. D **58**, 094021 (1998). All cross sections we quote are for a fixed top quark mass of 175 GeV/ c^2 .
- [4] M.C. Smith and S.S. Willenbrock, Phys. Rev. D **54**, 6696 (1996).
- [5] R. Bonciani *et al.*, Nucl. Phys. **B529**, 424 (1998). The authors cite $\sigma_{t\bar{t}} = 5.06^{+0.13}_{-0.36}$ pb at $\sqrt{s} = 1.8$ TeV for a top quark mass of 175 GeV/ c^2 . We use a linear plot to assess the effect on the cross section of the uncertainty on the top mass; in quadrature with the uncertainty above, this gives an uncertainty on $\sigma_{t\bar{t}}$ of $\sim 18\%$.
- [6] DØ Collaboration, V.M. Abazov *et al.*, Phys. Lett. B **517**, 282 (2001).
- [7] In the CDF coordinate system, θ is the polar angle with respect to the proton beam direction and ϕ is the azimuth. The pseudorapidity η is defined as $-\ln \tan(\theta/2)$. The transverse momentum of a particle is $P_T = P \sin \theta$ and its transverse energy is $E_T = E \sin \theta$.
- [8] F. Larios and C.-P. Yuan, Phys. Rev. D **55**, 7218 (1997).
- [9] G. Burdman, R.S. Chivukula, and N. Evans, Phys. Rev. D **62**, 075007 (2000).
- [10] J.L. Rosner and E. Takasugi, Phys. Rev. D **42**, 241 (1990); T.M.P. Tait and C.-P. Yuan, *ibid.* **63**, 014018 (2001).
- [11] F. Abe *et al.*, Nucl. Instrum. Methods Phys. Res. A **271**, 387 (1988); D. Amidei *et al.*, *ibid.* **350**, 73 (1994); P. Azzi *et al.*, *ibid.* **360**, 137 (1995).
- [12] A lepton is “isolated” if the nonlepton E_T in an η - ϕ cone of radius 0.4 centered on the lepton is less than 10% of the lepton’s E_T or P_T .
- [13] Missing transverse energy \cancel{E}_T is defined as the magnitude of $-\sum_i E_T^i \hat{n}_i$, where \hat{n}_i is a unit vector in the azimuthal plane that points from the beamline to the i th calorimeter tower.
- [14] CDF Collaboration, F. Abe *et al.*, Phys. Rev. Lett. **80**, 2779 (1998).
- [15] CDF Collaboration, F. Abe *et al.*, Phys. Rev. Lett. **79**, 3819 (1997).
- [16] This procedure generally yields two solutions for the neutrino P_z . We use the solution with the smallest absolute value. In cases where the solutions are complex conjugate, we use their real part.
- [17] T. Sjöstrand, Comput. Phys. Commun. **82**, 74 (1994). We use PYTHIA version 5.6.
- [18] G. Marchesini and B.R. Webber, Nucl. Phys. **B310**, 461 (1988); G. Marchesini *et al.*, Comput. Phys. Commun. **67**, 465 (1992). We use HERWIG version 5.6.
- [19] F.A. Berends, W.T. Giele, H. Kuijff, and B. Tausk, Nucl. Phys. **B357**, 32 (1991).